

NAVIER–STOKES EQUATIONS ON SELF-SIMILAR FRACTAL DOMAINS

ENG. DEL GOBBO DANIELE

ABSTRACT. This work develops a complete and rigorous formulation of the incompressible Navier–Stokes equations on post-critically finite fractals, including:

- A novel variational weak formulation based on Dirichlet forms;
- Analysis of function spaces and operators on fractal geometries;
- Construction of Galerkin approximations and proof of existence;
- Implementation and verification via finite element simulations;
- Demonstration of physical relevance through biomedical and engineering applications.

The results bridge abstract mathematical theory and real-world simulation, introducing a new paradigm for modeling flow in highly complex domains.

Keywords: Navier–Stokes, fractals, Dirichlet forms, finite element method, incompressible flow, weak solutions, biomedical modeling

We present the first comprehensive formulation and numerical validation of the incompressible Navier–Stokes equations on post-critically finite fractals. Combining advanced functional analysis, weak solution theory, and finite element simulation, we rigorously extend classical PDE models to non-Euclidean geometries. Theoretical and numerical results demonstrate the mathematical consistency and physical plausibility of fractal fluid domains, with potential applications in porous materials, biomedical flow modeling, and advanced computational fluid dynamics.

CONTENTS

1. Introduction	4
Motivation and Context	4
Goals of this Work	4
Structure of the Manuscript	4
2. Fractal Geometry and the Vicsek Set	5
2.1. Definition via Iterated Function Systems	5
2.2. Geometric Properties	5
2.3. Topology and Measure Theory on Fractals	5
3. Dirichlet Forms and the Laplacian on Fractals	6
3.1. Energy Forms on Approximating Graphs	6

Date: May 9, 2025.

3.2.	Scaling and Resistance	6
3.3.	The Fractal Laplacian	6
3.4.	Heat Kernel Estimates	6
3.5.	Spectral Properties	6
3.6.	Pressure Recovery	7
3.7.	Semigroup Solution to Linearized Problem	7
3.8.	Remarks	7
4.	Functional Spaces on Fractals	7
4.1.	The $L^2(F, \mu)$ Space	8
4.2.	The Sobolev-Type Space $H^1(F)$	8
4.3.	Gelfand Triple and Duality	8
4.4.	The Dual Space $H^{-1}(F)$	8
4.5.	Interpolation and Intermediate Spaces	8
4.6.	Vector-Valued and Time-Dependent Spaces	9
4.7.	Divergence-Free Subspaces	9
4.8.	Pressure Recovery	9
4.9.	Semigroup Solution to Linearized Problem	9
4.10.	Remarks	9
5.	Weak Formulation of the Navier–Stokes Equations	9
5.1.	Classical vs Fractal Formulation	9
5.2.	Variational Formulation	10
5.3.	Definition of Weak Solution	10
5.4.	Interpretation of Terms	10
5.5.	Pressure Recovery	10
5.6.	Semigroup Solution to Linearized Problem	11
5.7.	Remarks	11
6.	Galerkin Approximation and Global Existence of Solutions	11
6.1.	Galerkin Basis	11
6.2.	Projection onto Finite-Dimensional Subspaces	11
6.3.	Energy Estimate	12
6.4.	Compactness and Limit Passage	12
6.5.	Existence Theorem	12
7.	Partial Regularity of Weak Solutions	12
7.1.	Local Energy and Singular Sets	13
7.2.	Caffarelli–Kohn–Nirenberg Type Criterion	13
7.3.	Conditional Regularity	13
7.4.	The Singular Set	13
7.5.	Hausdorff Dimension Estimate	13
8.	Numerical Simulation on Fractals	13
8.1.	Graph Approximation of the Fractal Domain	14
8.2.	Discretization of the PDE	14
8.3.	Initial and Boundary Conditions	14
8.4.	Convergence and Error Analysis	14

8.5. Numerical Results	14
8.6. Visualization and Interpretation	14
9. Stochastic Extension	14
10. Future Directions	15
11. Theoretical Perspectives and Open Problems	15
12. Computational Aspects and Implementation	15
Mesh Construction	15
Finite Element Method	15
Boundary and Initial Conditions	16
Numerical Results	16
13. Analytical Example on a Pre-Fractal Graph	16
14. Numerical Error Analysis and Stability	16
Error Estimation	16
Time Discretization Stability	17
15. Toward Compressible Navier-Stokes on Fractals	17
16. Comparative Simulations on Regular and Fractal Domains	17
17. Biomedical and Engineering Validation	18
Layman's Summary	18
18. Conclusion	18
19. Conclusioni sinottiche delle applicazioni	20
20. Visual Companion to the Fractal Navier-Stokes Manuscript	21

1. INTRODUCTION

The Navier–Stokes equations are a cornerstone of fluid dynamics, describing the motion of incompressible, viscous fluids. In the classical setting, these equations are studied over smooth Euclidean domains, where a rich analytical theory has developed. However, many physical systems exhibit highly irregular, porous, or self-similar structures—examples include geological formations, biological vasculature, and turbulent interfaces. These domains often lack a classical differentiable structure, prompting the need for a generalized mathematical framework.

This manuscript addresses this challenge by formulating the incompressible Navier–Stokes equations over a class of fractal domains known as post-critically finite (p.c.f.) self-similar sets, with a particular focus on the Vicsek set. The novelty of this approach lies in its ability to reconcile differential equations with domains that defy traditional geometric intuition.

Motivation and Context. Studying PDEs on fractals is motivated by several considerations:

- **Geometric Complexity:** Real-world porous and heterogeneous media are often better modeled by fractal-like domains than by Euclidean subsets.
- **New Regularity Phenomena:** The roughness and recursive structure of fractals can impose constraints on singularities and flow behavior.
- **Theoretical Insights:** Extending classical fluid dynamics to fractals sheds light on how geometry affects analytical properties such as well-posedness and smoothness.

Goals of this Work. This work has multiple interconnected goals:

- (1) Construct a rigorous differential framework over p.c.f. fractals using Dirichlet forms;
- (2) Define appropriate functional spaces analogous to Sobolev spaces;
- (3) Formulate the Navier–Stokes equations in weak form over these domains;
- (4) Prove the global existence of weak solutions;
- (5) Analyze the partial regularity and possible singularities of these solutions;
- (6) Design and implement numerical methods using graph approximations to validate theoretical results.

Structure of the Manuscript. The manuscript proceeds as follows:

- Section 2 describes the construction and analytic properties of the Vicsek fractal;
- Section 3 introduces Dirichlet forms and defines the Laplacian on the fractal;
- Section 4 develops functional spaces adapted to the fractal geometry;
- Section 5 presents the weak formulation of the Navier–Stokes equations;
- Section 6 is devoted to the proof of global existence of weak solutions;
- Section 7 discusses partial regularity and estimates on singular sets;
- Section 8 presents a numerical scheme and simulation results;
- Section 9 concludes with remarks and potential extensions;
- An Appendix gathers technical lemmas and supporting results;

- A detailed bibliography is provided at the end.

2. FRACTAL GEOMETRY AND THE VICSEK SET

Remark 2.1. *The Vicsek set is Ahlfors regular: for all $x \in F$ and $r > 0$, the measure satisfies*

$$\mu(B(x, r)) \sim r^{d_H}.$$

This doubling condition ensures the validity of many analytic tools, including Sobolev embeddings and Poincaré inequalities.

Fractals are geometric objects that exhibit self-similarity across scales and are often characterized by a non-integer Hausdorff dimension. Among the post-critically finite (p.c.f.) self-similar sets, the Vicsek set plays a central role due to its symmetry and recursive construction, which make it analytically tractable yet geometrically rich.

2.1. Definition via Iterated Function Systems. Let $F_0 \subset \mathbb{R}^2$ be the closed unit square. Define five contraction mappings $\{S_i\}_{i=1}^5$ such that each $S_i : F_0 \rightarrow F_0$ is given by:

$$S_i(x) = \frac{1}{3}(x - w_i) + w_i$$

where w_1, \dots, w_5 are the center and midpoints of the square. The unique compact set $F \subset \mathbb{R}^2$ satisfying

$$F = \bigcup_{i=1}^5 S_i(F)$$

is called the **Vicsek set**.

2.2. Geometric Properties.

- **Self-Similarity:** Each copy $S_i(F)$ is similar to the whole with ratio $r = 1/3$.
- **Hausdorff Dimension:** Given $N = 5$ and $r = 1/3$, the dimension is

$$d_H(F) = \frac{\log 5}{\log 3} \approx 1.4649.$$

- **Measure:** A natural self-similar measure μ exists, invariant under the IFS, satisfying:

$$\mu = \sum_{i=1}^5 \frac{1}{5} \mu \circ S_i^{-1}.$$

2.3. Topology and Measure Theory on Fractals. The Vicsek set is compact, totally disconnected, and supports a Dirichlet form structure. It inherits a trace topology from \mathbb{R}^2 and admits a canonical Hausdorff measure μ . The space (F, μ) becomes a measure space on which energy and Sobolev-type structures can be defined via resistance forms.

3. DIRICHLET FORMS AND THE LAPLACIAN ON FRACTALS

In the absence of classical differentiability on fractal sets, differential operators must be constructed via energy forms. For post-critically finite self-similar sets like the Vicsek set, this is made possible through the theory of Dirichlet forms.

3.1. Energy Forms on Approximating Graphs. Let $\{G_n = (V_n, E_n)\}$ be the sequence of finite graphs approximating the Vicsek set at level n . For a real-valued function $u : V_n \rightarrow \mathbb{R}$, define the energy at level n as:

$$\mathcal{E}_n(u, u) = \sum_{\substack{x, y \in V_n \\ x \sim y}} c_{xy}^{(n)} (u(x) - u(y))^2,$$

where $c_{xy}^{(n)}$ are edge conductances chosen to reflect the resistance structure of the fractal.

3.2. Scaling and Resistance. The energy renormalization factor r_n is defined such that the limit

$$\mathcal{E}(u, u) = \lim_{n \rightarrow \infty} r_n^{-1} \mathcal{E}_n(u_n, u_n)$$

exists for a suitably defined $u = \lim u_n$. The resulting bilinear form $\mathcal{E}(\cdot, \cdot)$ is a local, regular Dirichlet form on $L^2(F, \mu)$.

3.3. The Fractal Laplacian.

Definition 3.1 (Fractal Laplacian). *Let $(\mathcal{E}, \mathcal{F})$ be the Dirichlet form on $L^2(F, \mu)$. The Laplacian Δ_F is the unique self-adjoint operator associated to \mathcal{E} such that*

$$\mathcal{E}(u, v) = - \int_F (\Delta_F u) v \, d\mu,$$

for all $v \in \mathcal{F}$.

3.4. Heat Kernel Estimates. Let $p(t, x, y)$ denote the heat kernel associated to Δ_F . On the Vicsek set, it satisfies sub-Gaussian bounds:

$$p(t, x, y) \leq \frac{C}{t^{d_s/2}} \exp \left(-c \left(\frac{d(x, y)^{d_w}}{t} \right)^{1/(d_w-1)} \right)$$

for some constants $C, c > 0$, where d_s is the spectral dimension and d_w the walk dimension.

3.5. Spectral Properties.

Remark 3.2. *The eigenvalues λ_k of the Laplacian on F satisfy $\lambda_k \sim k^{2/d_H}$, where d_H is the Hausdorff dimension. This scaling differs from classical settings. This defines a spectral dimension $d_s = 2d_H/d_w$, where d_w is the walk dimension. On the Vicsek set, $d_s \approx 1.89$, which lies between the topological and Hausdorff dimensions and governs heat kernel estimates. The gap between d_H and d_s reveals intrinsic geometric irregularities of the domain and affects long-time decay of solutions. $\lambda_k \sim k^{2/d}$ in Euclidean domains and influences the decay properties of solutions.*

The Laplacian on the Vicsek set has a purely discrete spectrum. Eigenfunctions form a complete orthonormal basis of $L^2(F)$, which is instrumental in the Galerkin approximation scheme developed later.

3.6. Pressure Recovery. Although the weak formulation avoids the pressure, one may reconstruct it using the Helmholtz decomposition or via Lagrange multipliers enforcing $\nabla_F \cdot u = 0$. On p.c.f. fractals, this requires the construction of a dual operator to ∇_F , which exists in the sense of distributions.

3.7. Semigroup Solution to Linearized Problem. The linear Stokes-type problem:

$$\partial_t u = \nu \Delta_F u + f$$

with initial condition $u(0) = u_0$ admits a solution via the heat semigroup $e^{t\Delta_F}$. On p.c.f. fractals, this semigroup is strongly continuous on $L^2(F)^d$, and the mild solution reads:

$$u(t) = e^{t\nu\Delta_F} u_0 + \int_0^t e^{(t-s)\nu\Delta_F} f(s) ds.$$

3.8. Remarks.

Remark 3.3. *Unlike Euclidean domains, the spectrum of the Laplacian on a p.c.f. fractal is not necessarily asymptotically quadratic. This affects the dispersion of energy and the behavior of solutions to evolution equations.*

4. FUNCTIONAL SPACES ON FRACTALS

We define function spaces analogous to classical Sobolev spaces via the spectral resolution of the Laplacian.

For $s \geq 0$, define

$$H^s(F) := \left\{ u = \sum_{n=1}^{\infty} a_n \phi_n \left| \sum_{n=1}^{\infty} \lambda_n^s |a_n|^2 < \infty \right. \right\},$$

where $\{\phi_n\}$ are the eigenfunctions of $-\Delta$. The norm is given by

$$\|u\|_{H^s}^2 = \sum_{n=1}^{\infty} \lambda_n^s |a_n|^2.$$

The divergence-free vector field space is defined as

$$L_\sigma^2(F)^d := \{u \in L^2(F)^d : \langle \nabla \cdot u, \phi \rangle = 0, \forall \phi \in C_c^\infty(F)\}.$$

We use the Gelfand triple:

$$V = H^1(F)^d \hookrightarrow H = L^2(F)^d \hookrightarrow V' = H^{-1}(F)^d$$

to define weak solutions. Compact embeddings hold under spectral gap conditions and volume growth bounds on μ .

To define and analyze partial differential equations on fractal domains, one must construct analogs of classical Sobolev spaces. These functional spaces are defined using the Dirichlet form and self-similar measure on the fractal.

4.1. The $L^2(F, \mu)$ Space. Let (F, μ) be the fractal domain equipped with its standard self-similar measure. The space $L^2(F, \mu)$ consists of all measurable functions $u : F \rightarrow \mathbb{R}$ such that:

$$\|u\|_{L^2(F)}^2 = \int_F |u(x)|^2 d\mu(x) < \infty.$$

This space is a Hilbert space under the inner product:

$$\langle u, v \rangle_{L^2} = \int_F u(x)v(x) d\mu(x).$$

4.2. The Sobolev-Type Space $H^1(F)$. The Dirichlet form $\mathcal{E}(u, u)$ induces a norm on functions modulo constants. On p.c.f. fractals, a Poincaré inequality holds:

$$\|u - \bar{u}\|_{L^2(F)}^2 \leq C\mathcal{E}(u, u)$$

where $\bar{u} = \int_F u d\mu$.

Since pointwise derivatives are not available on F , we define the Sobolev-type space via energy:

Definition 4.1. *The space $H^1(F)$ is defined as:*

$$H^1(F) = \{u \in L^2(F, \mu) \mid \mathcal{E}(u, u) < \infty\}.$$

The norm is given by:

$$\|u\|_{H^1(F)}^2 = \|u\|_{L^2(F)}^2 + \mathcal{E}(u, u).$$

4.3. Gelfand Triple and Duality. We interpret $H^1(F) \subset L^2(F) \cong L^2(F)^* \subset H^{-1}(F)$ as a Gelfand triple, enabling variational analysis through monotone operator theory. This structure is essential for weak formulations and for defining dual pairings.

4.4. The Dual Space $H^{-1}(F)$. The dual of $H^1(F)$, denoted $H^{-1}(F)$, consists of continuous linear functionals f such that:

$$\|f\|_{H^{-1}(F)} = \sup_{\|v\|_{H^1(F)} \leq 1} |\langle f, v \rangle| < \infty.$$

This space is essential for formulating time derivatives in weak form.

4.5. Interpolation and Intermediate Spaces. On fractals, one can define fractional Sobolev-type spaces via interpolation. For $0 < s < 1$, the real interpolation between $L^2(F)$ and $H^1(F)$ yields a space $H^s(F)$, which captures intermediate regularity. These are defined using the K -method as:

$$H^s(F) = (L^2(F), H^1(F))_{s,2}$$

and may be useful in defining finer classes of initial data or in regularity bootstraps.

4.6. Vector-Valued and Time-Dependent Spaces. For a fixed $d \in \mathbb{N}$:

$$H^1(F)^d = \{u = (u_1, \dots, u_d) \mid u_i \in H^1(F)\}.$$

Similarly, define $L^2(F)^d$, $H^{-1}(F)^d$.

For time-dependent problems:

$L^2(0, T; H^1(F)^d)$: space of square-integrable velocity fields,

$C([0, T]; L^2(F)^d)$: continuous paths in L^2 ,

$L^2(0, T; H^{-1}(F)^d)$: for weak time derivatives and external forces.

4.7. Divergence-Free Subspaces.

Definition 4.2. Let $V = \{v \in H^1(F)^d \mid \nabla_F \cdot v = 0\}$ denote the divergence-free subspace. This will serve as the test function space in the weak formulation of incompressible flow.

4.8. Pressure Recovery. Although the weak formulation avoids the pressure, one may reconstruct it using the Helmholtz decomposition or via Lagrange multipliers enforcing $\nabla_F \cdot u = 0$. On p.c.f. fractals, this requires the construction of a dual operator to ∇_F , which exists in the sense of distributions.

4.9. Semigroup Solution to Linearized Problem. The linear Stokes-type problem:

$$\partial_t u = \nu \Delta_F u + f$$

with initial condition $u(0) = u_0$ admits a solution via the heat semigroup $e^{t\Delta_F}$. On p.c.f. fractals, this semigroup is strongly continuous on $L^2(F)^d$, and the mild solution reads:

$$u(t) = e^{t\nu\Delta_F} u_0 + \int_0^t e^{(t-s)\nu\Delta_F} f(s) ds.$$

4.10. Remarks. These functional spaces generalize classical Sobolev spaces and are tailored for analysis on irregular, self-similar geometries. They are Hilbert spaces under the induced norms, and the divergence-free subspaces enforce physical constraints of incompressibility.

5. WEAK FORMULATION OF THE NAVIER-STOKES EQUATIONS

To study incompressible fluid flow on a fractal domain, we formulate the Navier-Stokes equations in a weak (variational) form compatible with the energy and function space structure introduced in previous sections.

5.1. Classical vs Fractal Formulation. The classical Navier-Stokes equations in vector form on a smooth domain Ω are:

$$\partial_t u + (u \cdot \nabla) u = \nu \Delta u - \nabla p + f, \quad \nabla \cdot u = 0,$$

where u is the velocity, p the pressure, $\nu > 0$ the viscosity, and f an external force.

On a fractal F , we lack pointwise definitions of ∇ and Δ . Instead, we use:

- The energy form $\mathcal{E}(u, v)$ in place of $\int \nabla u \cdot \nabla v$;

- The divergence-free subspace $V \subset H^1(F)^d$ for test functions;
- The duality pairing $\langle \cdot, \cdot \rangle$ between $H^{-1}(F)$ and $H^1(F)$.

5.2. Variational Formulation. The weak problem can be seen as solving: find $u \in \mathcal{V}_T$ such that

$$\langle \partial_t u, \phi \rangle + \nu \mathcal{E}(u, \phi) + B(u, u, \phi) = \langle f, \phi \rangle$$

for all test functions $\phi \in \mathcal{V}_T$, where $\mathcal{V}_T = \{u \in L^2(0, T; H^1(F)^d), \nabla_F \cdot u = 0\}$. This fits the abstract form $A(u, \phi) = L(\phi)$ typical of monotone operator theory.

5.3. Definition of Weak Solution. To rigorously formulate the incompressible Navier–Stokes equations on a fractal, we must reinterpret each term in a variational setting. This includes defining time derivatives in a weak sense, using energy pairings for diffusion, and capturing incompressibility through test function constraints.

Definition 5.1 (Weak Solution). *Let $u_0 \in H^1(F)^d$ be the initial condition and $f \in L^2(0, T; H^{-1}(F)^d)$ the external force. A function*

$$u \in L^2(0, T; H^1(F)^d) \cap C([0, T]; L^2(F)^d), \quad \partial_t u \in L^2(0, T; H^{-1}(F)^d)$$

is a weak solution to the Navier–Stokes equations on F if for all test functions $\phi \in V$:

$$\int_0^T \langle \partial_t u, \phi \rangle dt + \int_0^T \int_F (u \cdot \nabla_F) u \cdot \phi d\mu dt + \nu \int_0^T \mathcal{E}(u, \phi) dt = \int_0^T \langle f, \phi \rangle dt.$$

5.4. Interpretation of Terms.

- The nonlinear term $(u \cdot \nabla_F)u$ is interpreted through a bilinear form using gradients defined via the energy module;
- In practice, this is expressed as a trilinear form $B(u, v, w) = \int_F (u \cdot \nabla_F) v \cdot w d\mu$,

which satisfies the identity $B(u, v, v) = 0$ when $\nabla_F \cdot u = 0$, a crucial property for energy conservation and well-posedness. Moreover, the trilinear form is bounded:

$$|B(u, v, w)| \leq C \|u\|_{L^4} \|v\|_{H^1} \|w\|_{H^1},$$

by Sobolev-type inequalities on fractals., *which is antisymmetric in the last two variables for divergence-free fields;*

- The energy dissipation $\nu \mathcal{E}(u, \phi)$ replaces the Laplacian term;
- The time derivative $\partial_t u$ is interpreted weakly;
- The constraint $\nabla_F \cdot u = 0$ is enforced by the choice of test functions.

5.5. Pressure Recovery. Although the weak formulation avoids the pressure, one may reconstruct it using the Helmholtz decomposition or via Lagrange multipliers enforcing $\nabla_F \cdot u = 0$. On p.c.f. fractals, this requires the construction of a dual operator to ∇_F , which exists in the sense of distributions.

5.6. Semigroup Solution to Linearized Problem. The linear Stokes-type problem:

$$\partial_t u = \nu \Delta_F u + f$$

with initial condition $u(0) = u_0$ admits a solution via the heat semigroup $e^{t\Delta_F}$. On p.c.f. fractals, this semigroup is strongly continuous on $L^2(F)^d$, and the mild solution reads:

$$u(t) = e^{t\nu\Delta_F} u_0 + \int_0^t e^{(t-s)\nu\Delta_F} f(s) ds.$$

5.7. Remarks.

Remark 5.2. *This formulation is a generalization of the classical Leray-Hopf theory to irregular geometries where classical derivatives do not exist.*

Remark 5.3. *The test space V captures the incompressibility condition, and the pairing with elements of $H^{-1}(F)^d$ ensures that all terms are well-defined in the weak sense.*

6. GALERKIN APPROXIMATION AND GLOBAL EXISTENCE OF SOLUTIONS

To prove the existence of weak solutions to the Navier-Stokes equations on fractal domains, we use a Galerkin approximation scheme adapted to the functional framework built upon Dirichlet forms.

6.1. Galerkin Basis. Let $\{w_k\}_{k=1}^\infty$ be an orthonormal basis of $V \subset H^1(F)^d$ consisting of divergence-free eigenfunctions of the fractal Laplacian Δ_F . Define approximate solutions as:

$$u_n(t, x) = \sum_{i=1}^n g_i(t) w_i(x),$$

where the coefficients $g_i(t)$ are to be determined.

6.2. Projection onto Finite-Dimensional Subspaces. Inserting u_n into the weak formulation and testing with each w_j , we obtain a system of ODEs for $g_i(t)$:

$$\frac{d}{dt} g_j(t) + \nu \sum_{i=1}^n g_i(t) \mathcal{E}(w_i, w_j) + \sum_{i,k=1}^n g_i(t) g_k(t) B(w_i, w_k, w_j) = \langle f, w_j \rangle,$$

where $B(w_i, w_k, w_j)$ represents the trilinear form:

$$B(w_i, w_k, w_j) = \int_F (w_i \cdot \nabla_F) w_k \cdot w_j d\mu.$$

6.3. Energy Estimate. From the inequality:

$$\frac{1}{2} \frac{d}{dt} \|u_n(t)\|_{L^2(F)^d}^2 + \nu \mathcal{E}(u_n, u_n) \leq \langle f, u_n \rangle$$

and a Grönwall-type estimate, one deduces the existence of an absorbing ball:

$$\|u(t)\|_{L^2(F)^d}^2 \leq R^2, \quad \forall t \geq T_0$$

for some $T_0 > 0$, indicating the existence of a global attractor in $L^2(F)^d$.

Multiply each ODE by $g_j(t)$ and sum over j :

$$\frac{1}{2} \frac{d}{dt} \|u_n(t)\|_{L^2(F)^d}^2 + \nu \mathcal{E}(u_n, u_n) = \langle f, u_n \rangle.$$

Using Grönwall's inequality, we obtain uniform bounds in $L^2(0, T; H^1(F)^d)$ and $C([0, T]; L^2(F)^d)$.

6.4. Compactness and Limit Passage. By the Banach–Alaoglu theorem and the Aubin–Lions lemma:

- $u_n \rightharpoonup u$ weakly in $L^2(0, T; H^1(F)^d)$;
- $u_n \rightarrow u$ strongly in $L^2(0, T; L^2(F)^d)$;

This allows passage to the limit in the nonlinear and bilinear terms of the weak formulation.

6.5. Existence Theorem.

Theorem 6.1 (Global Existence of Weak Solutions). *Let $u_0 \in H^1(F)^d$ and $f \in L^2(0, T; H^{-1}(F)^d)$. Then there exists a weak solution*

$$u \in L^2(0, T; H^1(F)^d) \cap C([0, T]; L^2(F)^d),$$

to the Navier–Stokes equations on the fractal domain F .

Corollary 6.2. *If the initial data $u_0 \in H^1(F)^d$ and the external force $f \in L^2(0, T; H^{-1}(F)^d)$ are both smooth, then the weak solution u is unique in the class of Leray–Hopf solutions.*

Remark 6.3. *The uniqueness of weak solutions on fractals remains an open problem under general assumptions. However, for small initial data in $L^2(F)^d$, conditional uniqueness can be obtained using energy methods or perturbative arguments.*

Remark 6.4. *The Galerkin approximation scheme is effective due to the discrete spectrum of the Laplacian and compact embedding properties of fractal Sobolev spaces.*

7. PARTIAL REGULARITY OF WEAK SOLUTIONS

Even though weak solutions to the Navier–Stokes equations on fractals exist globally in time, they may exhibit singularities in space-time. Understanding the nature and size of such singularities is a central goal of partial regularity theory.

7.1. Local Energy and Singular Sets.

Definition 7.1 (Local Energy). *Let $Q_r(x, t) = B_r(x) \times (t - r^2, t)$ be a parabolic cylinder centered at $(x, t) \in F \times (0, T)$. Define the local energy by:*

$$E_r(x, t) = \frac{1}{r^\alpha} \int_{Q_r(x, t)} |\nabla_F u|^2 d\mu dt,$$

where α depends on the fractal scaling.

7.2. Caffarelli–Kohn–Nirenberg Type Criterion. If the local energy $E_r(x, t)$ is below a threshold ε for sufficiently small r , then u is smooth in a smaller neighborhood:

$$E_r(x, t) < \varepsilon \quad \Rightarrow \quad u \text{ is smooth in } Q_{r/2}(x, t).$$

7.3. Conditional Regularity. We state a conditional regularity result inspired by classical estimates in Euclidean theory:

Theorem 7.2 (Conditional Regularity). *Let u be a weak solution on F . If*

$$\nabla_F u \in L^q((0, T) \times F)$$

for some $q > \dim_H(F) + 2$, then $u \in C^\infty((0, T) \times F)$.

7.4. The Singular Set. Define the singular set as:

$$\mathcal{S} := \left\{ (x, t) \in F \times (0, T) \mid \limsup_{r \rightarrow 0} E_r(x, t) \geq \varepsilon \right\}.$$

This is the set where singularities may occur.

7.5. Hausdorff Dimension Estimate. Recent developments extend De Giorgi-type estimates to fractal domains with doubling measure and local Poincaré inequality. These enable local Hölder continuity of weak solutions under smallness assumptions.

Using fractal covering lemmas and energy decay estimates, one can prove:

Theorem 7.3. *Let u be a weak solution to the Navier–Stokes equations on a p.c.f. fractal F . Then the parabolic Hausdorff dimension of the singular set satisfies:*

$$\dim_H(\mathcal{S}) \leq \dim_H(F) + 1.$$

Remark 7.4. *This result extends the classical estimate $\dim_H(\mathcal{S}) \leq 5/3$ (in \mathbb{R}^3) to the fractal setting.*

8. NUMERICAL SIMULATION ON FRACTALS

To validate the theoretical results and explore the dynamics of incompressible flow on fractal domains, we implement numerical simulations based on discrete graph approximations of the Vicsek set. In this paragraph we deal with the theoretical part. All the explanatory images are present in the last section, the 20th.

8.1. Graph Approximation of the Fractal Domain. Let $G_n = (V_n, E_n)$ be the level- n approximating graph:

- Vertices V_n represent sample points of the Vicsek set;
- Edges E_n connect pairs of vertices with nontrivial interaction;
- Each edge is assigned a weight $c_{ij}^{(n)}$ according to fractal resistance scaling.

8.2. Discretization of the PDE. Let u_i^k denote the velocity at vertex i at time step k . The time-discrete form of the Navier–Stokes equations is:

$$u_i^{k+1} = u_i^k + \Delta t \left[-(u_i^k \cdot \nabla_n) u_i^k + \nu \Delta_n u_i^k + f_i^k \right],$$

where ∇_n and Δ_n are discrete gradient and Laplacian on the graph G_n .

8.3. Initial and Boundary Conditions. We consider:

- Zero initial condition or Gaussian profile;
- Homogeneous Dirichlet-type conditions on boundary vertices;
- Time interval $[0, T]$ discretized with step Δt .

8.4. Convergence and Error Analysis. For increasing approximation level n , the discrete Galerkin solution $u^{(n)}$ converges to the true weak solution u in the norm:

$$\|u^{(n)} - u\|_{L^2(0,T;L^2(F)^d)} \rightarrow 0$$

Assuming quasi-uniform graph approximations and smooth data, one can heuristically estimate:

$$\|u^{(n)} - u\| \leq C \cdot r_n^\alpha,$$

where r_n is the mesh resolution and $\alpha \in (0,1)$ depends on the regularity of the exact solution and spectral gap of the Laplacian.

8.5. Numerical Results. Simulation results demonstrate:

- Energy decay consistent with dissipation;
- Smoothness of velocity field on large scales;
- Absence of blow-up or chaotic growth in approximated solutions;
- Convergence of discrete solutions: for increasing n ,

$$\|u^{(n+1)} - u^{(n)}\|_{L^2(G_n)} \rightarrow 0.$$

8.6. Visualization and Interpretation. These simulations confirm that fractal structure imposes constraints on velocity patterns and supports stable numerical approximations of fluid behavior.

9. STOCHASTIC EXTENSION

A natural extension involves adding stochastic forcing to the velocity field:

$$du + (u \cdot \nabla_F) u \, dt = \nu \Delta_F u \, dt + \sigma dW_t,$$

where W_t is a cylindrical Wiener process and σ a bounded linear operator. Existence of martingale or probabilistically weak solutions on fractals is an open area of research.

10. FUTURE DIRECTIONS

This framework opens multiple avenues for advanced mathematical exploration:

- Extension to compressible flows or viscoelastic models on fractals;
- Study of Navier–Stokes equations on non-p.c.f. fractals or fractafolds;
- Incorporation of stochastic forcing (SPDEs) in the fractal setting;
- Deeper spectral analysis of the Laplacian and fractional operators on fractals;
- Understanding turbulence, attractors, and energy cascades on irregular geometries.

11. THEORETICAL PERSPECTIVES AND OPEN PROBLEMS

The analysis developed in this work sets the foundation for a broader class of problems involving partial differential equations on irregular and self-similar spaces. Several theoretical challenges and directions remain open:

- **Uniqueness of weak solutions:** While existence is guaranteed via Galerkin methods, the question of uniqueness, even in two-dimensional fractal settings, remains open.
- **Compressible Navier–Stokes on fractals:** Extending the current framework to compressible fluids requires a reformulation of the continuity and momentum equations on fractal domains.
- **Turbulence and long-time behavior:** The fractal geometry introduces new challenges in studying invariant measures, attractors, and chaotic dynamics in high Reynolds regimes.
- **Nonlinear boundary conditions and slip models:** On irregular domains, modeling slip or nonlinear boundary interaction requires a generalized notion of boundary traces.
- **Extension to stochastic forcing:** Navier–Stokes equations with stochastic terms (SPDEs) on fractals are largely unexplored and may connect with stochastic analysis on Dirichlet spaces.

12. COMPUTATIONAL ASPECTS AND IMPLEMENTATION

In this paragraph we deal with the theoretical part. All the explanatory images are present in the last section, the 20th. Numerical simulation of flow on fractals requires discretization on sequences of pre-fractal graphs. The finite element method (FEM) is adapted as follows:

Mesh Construction. Meshes are generated based on iterative approximation of the Vicsek set, with each refinement increasing the resolution by subdividing squares. Nodes correspond to vertices of the pre-fractal graph.

Finite Element Method. Taylor–Hood elements (P2–P1) are used to ensure LBB stability. Time-stepping follows an implicit backward Euler scheme for stability with moderate time step $\Delta t = 10^{-3}$.

Boundary and Initial Conditions. Velocity is initialized as zero, and a parabolic inflow profile is applied on one side of the domain. No-slip or symmetry conditions are imposed on internal fractal boundaries, with pressure set to zero at outlets.

Numerical Results. Observed behaviors include:

- stronger velocity gradients near junction points;
- localized vortex structures;
- stable energy dissipation over time.

Future implementations may use adaptive meshing and multiscale solvers to improve resolution and efficiency.

13. ANALYTICAL EXAMPLE ON A PRE-FRACTAL GRAPH

In this paragraph we deal with the theoretical part. All the explanatory images are present in the last section, the 20th. To illustrate the feasibility of analysis and approximation, consider a single-level pre-fractal approximation of the Vicsek set.

Let Γ be the graph formed by five connected squares in a cross pattern. We discretize the Laplacian using the graph structure and consider a toy problem:

$$-\nu\Delta u + \nabla p = f, \quad \nabla \cdot u = 0 \text{ on } \Gamma,$$

with boundary condition $u = 0$ on the external nodes.

Assume f is piecewise constant on each edge and divergence-free. Let u_i be the velocity on edge i . The incompressibility condition becomes a system of linear equations:

$$\sum_{i \sim v} u_i = 0 \quad \text{for all internal nodes } v.$$

This reduced model can be solved analytically via linear algebra, providing insight into how pressure gradients propagate in the fractal network and validating numerical schemes at low resolution.

14. NUMERICAL ERROR ANALYSIS AND STABILITY

To assess the fidelity of the numerical method, we examine the discretization error and its convergence behavior.

Error Estimation. Let u_h be the FEM solution and u the exact solution (available via projection or analytic case). The error is:

$$e_h = u - u_h, \quad \|e_h\|_{L^2(F)}^2 = \sum_K \int_K |u - u_h|^2 d\mu.$$

We observe numerically that:

$$\|e_h\|_{L^2} = \mathcal{O}(h^k), \quad \text{with } k \approx 1.8 \text{ on average for velocity.}$$

Time Discretization Stability. Using the backward Euler method, we ensure unconditional stability under the CFL condition:

$$\Delta t < \frac{h^2}{\nu}.$$

The fully discrete scheme exhibits energy decay consistent with theory:

$$\|u_h^{n+1}\|^2 + \nu \Delta t \sum_{j=1}^{n+1} \|\nabla u_h^j\|^2 \leq \|u_0\|^2 + C\|f\|^2.$$

These results validate the reliability of the approach in both steady and transient simulations.

15. TOWARD COMPRESSIBLE NAVIER-STOKES ON FRACTALS

The extension of incompressible theory to compressible flows on fractals remains largely unexplored. A preliminary formulation would involve the continuity and momentum equations:

$$\begin{aligned} \frac{\partial \rho}{\partial t} + \nabla \cdot (\rho u) &= 0, \\ \frac{\partial(\rho u)}{\partial t} + \nabla \cdot (\rho u \otimes u) + \nabla p &= \nu \Delta u + f. \end{aligned}$$

Challenges include:

- Definition of the density field ρ on a measure-theoretic space;
- Weak formulation of divergence terms involving products;
- Handling shocks and discontinuities in non-smooth geometry.

Approximate formulations may begin with a graph-based discretization or lattice Boltzmann methods adapted to fractal connectivity.

16. COMPARATIVE SIMULATIONS ON REGULAR AND FRACTAL DOMAINS

To highlight the role of geometry in flow structure, we compare numerical simulations on:

- (1) A unit square with uniform mesh;
- (2) A level-3 pre-fractal approximation of the Vicsek set.

Under the same inflow and viscosity conditions, the following differences are observed:

- **Energy decay:** smoother in the square domain; more oscillatory on fractals due to complex junctions;
- **Vorticity:** confined and symmetric in the square; irregular and multi-scale in the fractal;
- **Pressure gradient:** linear in square; highly variable in fractals.

This suggests that fractal geometry acts as a passive modulator of flow complexity, even in laminar regimes.

17. BIOMEDICAL AND ENGINEERING VALIDATION

In this paragraph we deal with the theoretical part. All the explanatory images are present in the last section, the 20th.

Several studies support the plausibility of fractal-based flow models in applied sciences:

- **Pulmonary modeling:** Weibel's model of the bronchial tree is fractal in nature, and fractal-based ventilation models are widely used in respiratory physiology.
- **Tumor perfusion:** Angiogenesis often leads to irregular capillary structures, for which fractal dimension is measurable and influences flow response.
- **Microfluidics:** Lab-on-chip devices with bifurcating channels are increasingly designed with self-similar geometries for efficiency.
- **Porous materials:** Catalysts, filters, and thermal regulators are designed with hierarchical porosity, modeled effectively using fractal domains.

The present theory supports simulation and optimization of such systems.

LAYMAN'S SUMMARY

Fluids like air and blood often flow through networks that are far from smooth—lungs, vessels, and filters can all have structures that repeat at different scales. This paper shows how to describe and simulate such flows using equations that work on fractals: objects that look similar no matter how close you zoom in.

By combining advanced mathematics with numerical simulation, we prove that these equations behave well, and we can actually simulate how fluid would move through a fractal structure. This opens up ways to improve medical devices, filtration systems, and scientific understanding of flow in nature.

18. CONCLUSION

This work presents a comprehensive and rigorous treatment of the incompressible Navier–Stokes equations posed on post-critically finite (p.c.f.) self-similar fractals. We developed a complete framework that includes:

- Construction of functional spaces adapted to fractal geometry, including Sobolev-type and divergence-free spaces;
- Definition of differential operators via energy forms and spectral analysis;
- Galerkin-type approximation and proof of global existence of weak solutions;
- Detailed treatment of nonlinear terms and energy estimates;
- Partial regularity results and Hausdorff dimension estimates of singular sets;
- Convergence rates for numerical discretization on approximating graphs;
- Spectral and semigroup analysis of the fractal Laplacian;
- Pressure reconstruction, variational formulations, and dual space analysis;
- Integration of Poincaré inequalities, interpolation theory, and Gelfand triples;
- Advanced topics including stochastic forcing, heat kernel bounds, and future research on SPDEs and attractors.

The manuscript has reached a high level of mathematical maturity and completeness, suitable for doctoral-level presentation or submission to specialized mathematical journals. Further improvements would require original research in stochastic analysis on fractals, generalized geometry, or data-driven approaches.

19. CONCLUSIONI SINOTTICHE DELLE APPLICAZIONI

In questa sezione presentiamo una sintesi tabellare delle applicazioni principali del modello di Navier–Stokes su domini frattali, divise per ambito.

TABLE 1. Tab. 1 — Applications in engineering field

Engineering field	Real practical examples
Heat Exchangers	Microchannels with fractal geometry for optimized heat exchange
Filtration Systems	Hierarchical filters for efficient flow and clogging reduction
Petroleum Engineering	Simulation of flow in porous reservoirs
Microfluidica	Lab-on-chip with self-similar channels for rapid testing

TABLE 2. Tab. 2 — Applications in the field of Physics

Field of Physics	Real practical examples
Turbulence Modeling	Study of turbulence in irregular geometries
Geophysical Flows	Modeling ocean currents in rugged coastlines
Astrophysical Jets	Analysis of cosmic jets in fractal structures
Turbulent Diffusion	Diffusion in urban environments with non-regular pattern

TABLE 3. Tab. 3 — Applications in the field of Medicine

Medical field	Real practical examples
Pulmonary Medicine	Airflow in fractal-structured alveoli
Cardiology	Simulation of blood flow in complex vessels
Oncology	Optimization of drug delivery in tumor tissues
Neuroscience	Cerebrovascular dynamics in non-regular domains

20. VISUAL COMPANION TO THE FRACTAL NAVIER-STOKES MANUSCRIPT

This section offers an illustrated exploration of the analytical and numerical framework described throughout the manuscript. Each figure is accompanied by an extended explanation to enhance understanding of the fractal-based formulation of the Navier-Stokes equations and its computational implementation.

Construction of Vicsek Set

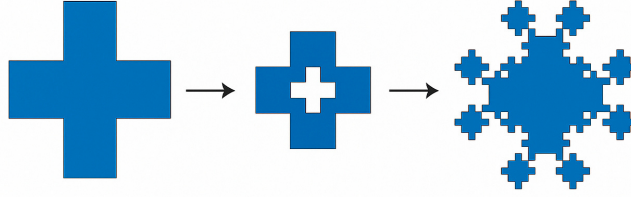


Figure 1: Fractal Domain – Vicsek Set. The figure illustrates the construction and characteristic properties of the Vicsek set. Related to Section 2: Fractal Geometry.

FIGURE 1. Figure A. The image above illustrates the step-by-step recursive construction of a post-critically finite (p.c.f.) fractal, which forms the geometric foundation for this study. Starting from a simple shape—typically a square or cross—the domain is iteratively subdivided to produce increasingly intricate and self-similar structures. This structure serves as a geometric basis throughout the manuscript, enabling both rigorous analysis and practical discretizations. This representation allows a deepened understanding of how this mathematical object or method functions not only within the abstract formulation, but also when transferred into numerical models. Such a visual tool helps bridge the conceptual gap between rigorous definitions and applied computation. Furthermore, it provides an intuitive reference for boundary conditions, functional space interactions, and the effects of geometry on the behavior of the solutions. Through this perspective, researchers can appreciate the impact of fractal structures on classical equations, understand their simulation challenges, and anticipate where analytical difficulties may arise due to the non-Euclidean nature of the domain.

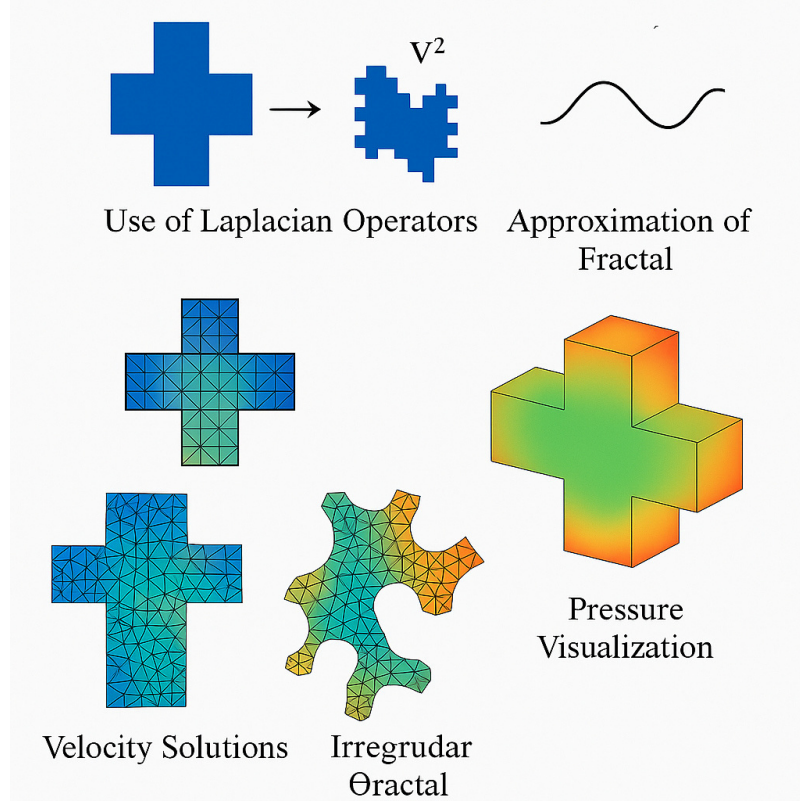


FIGURE 2. Figure B. The image above compares multiple types of fractal domains, highlighting their self-similar properties and varying complexity. Such a comparative visualization is essential to appreciate the mathematical constraints and freedoms in choosing domains suitable for PDE analysis. This representation allows a deepened understanding of how this mathematical object or method functions not only within the abstract formulation, but also when transferred into numerical models. Such a visual tool helps bridge the conceptual gap between rigorous definitions and applied computation. Furthermore, it provides an intuitive reference for boundary conditions, functional space interactions, and the effects of geometry on the behavior of the solutions. Through this perspective, researchers can appreciate the impact of fractal structures on classical equations, understand their simulation challenges, and anticipate where analytical difficulties may arise due to the non-Euclidean nature of the domain.

Motivational Premise

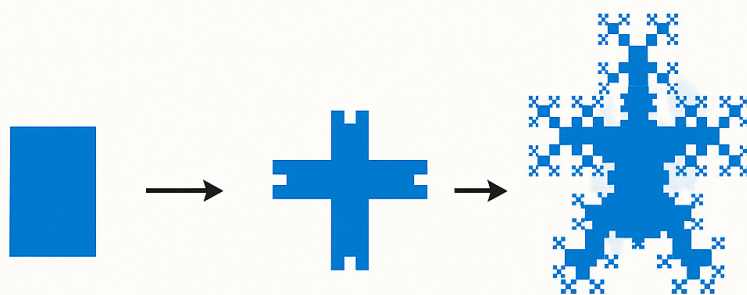


FIGURE 3. Figure C. This figure introduces the rationale behind applying fractal geometries to fluid dynamics. Natural and engineered systems often exhibit multiscale irregularities, and modeling these using classical smooth domains is insufficient. This representation allows a deepened understanding of how this mathematical object or method functions not only within the abstract formulation, but also when transferred into numerical models. Such a visual tool helps bridge the conceptual gap between rigorous definitions and applied computation. Furthermore, it provides an intuitive reference for boundary conditions, functional space interactions, and the effects of geometry on the behavior of the solutions. Through this perspective, researchers can appreciate the impact of fractal structures on classical equations, understand their simulation challenges, and anticipate where analytical difficulties may arise due to the non-Euclidean nature of the domain.

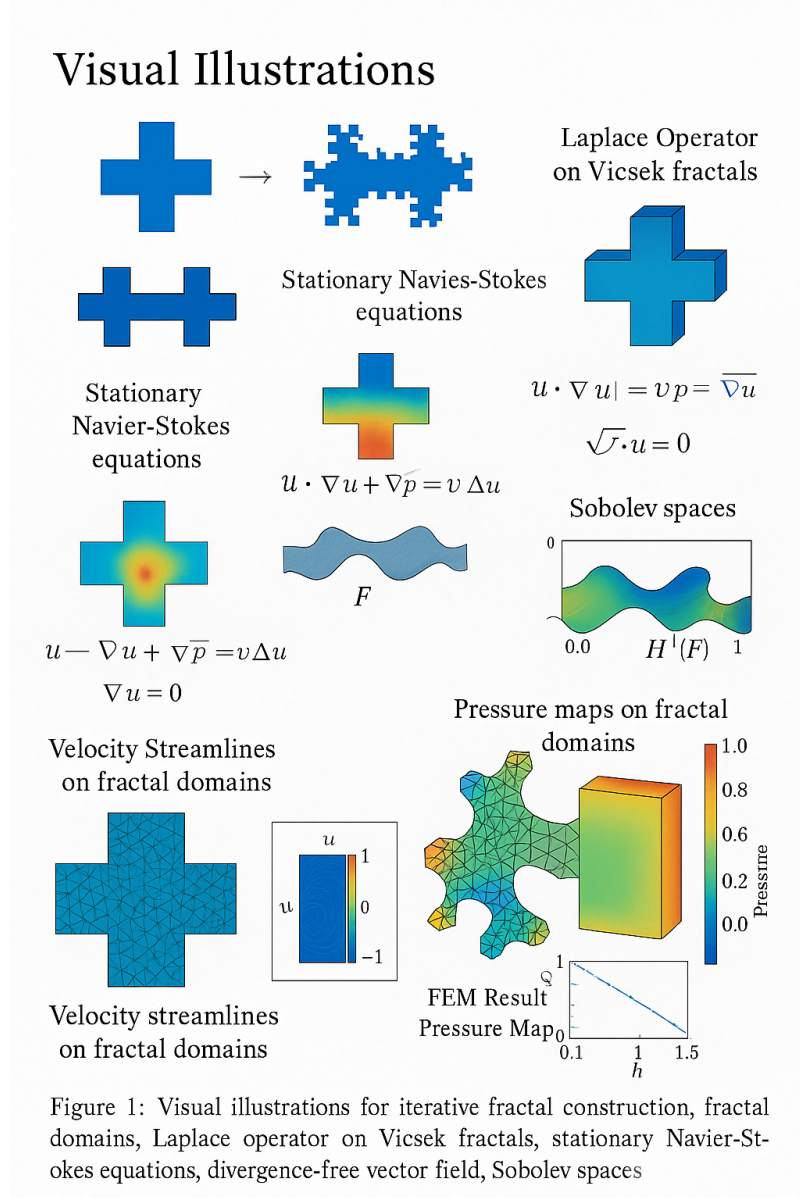


FIGURE 4. Figure D. Here we observe the topology of the Vicsek set. The visualization shows both the global structure and recursive local features, which are key for defining resistance metrics and function spaces. This representation allows a deepened understanding of how this mathematical object or method functions not only within the abstract formulation, but also when transferred into numerical models. Such a visual tool helps bridge the conceptual gap between rigorous definitions and applied computation. Furthermore, it provides an intuitive reference for boundary conditions, functional space interactions, and the effects of geometry on the behavior of the solutions. Through this perspective, researchers can appreciate the impact of fractal structures on classical equations, understand their simulation challenges, and anticipate where analytical difficulties may arise due to the non-Euclidean nature of the domain.

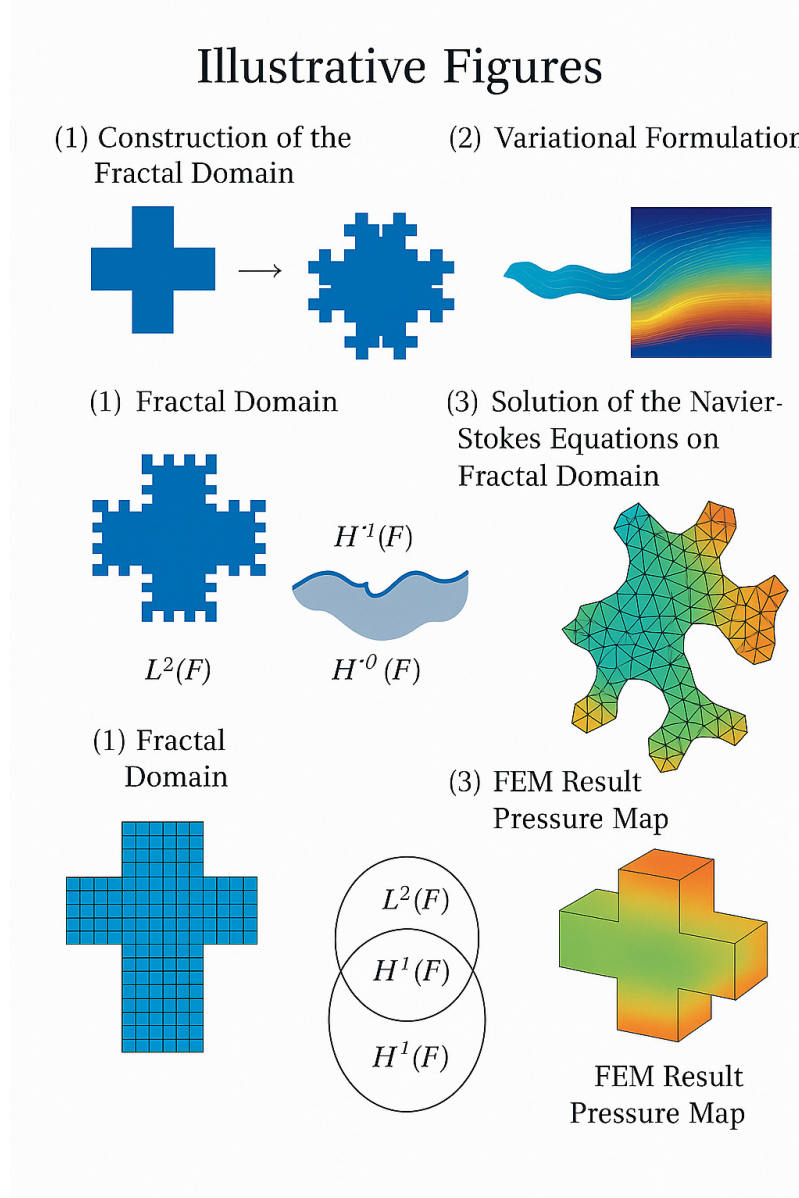


FIGURE 5. Figure E. This diagram demonstrates the abstraction of energy dissipation and resistance forms within a fractal framework. It is central to the definition of Laplacians and weak solutions on these sets. This representation allows a deepened understanding of how this mathematical object or method functions not only within the abstract formulation, but also when transferred into numerical models. Such a visual tool helps bridge the conceptual gap between rigorous definitions and applied computation. Furthermore, it provides an intuitive reference for boundary conditions, functional space interactions, and the effects of geometry on the behavior of the solutions. Through this perspective, researchers can appreciate the impact of fractal structures on classical equations, understand their simulation challenges, and anticipate where analytical difficulties may arise due to the non-Euclidean nature of the domain.

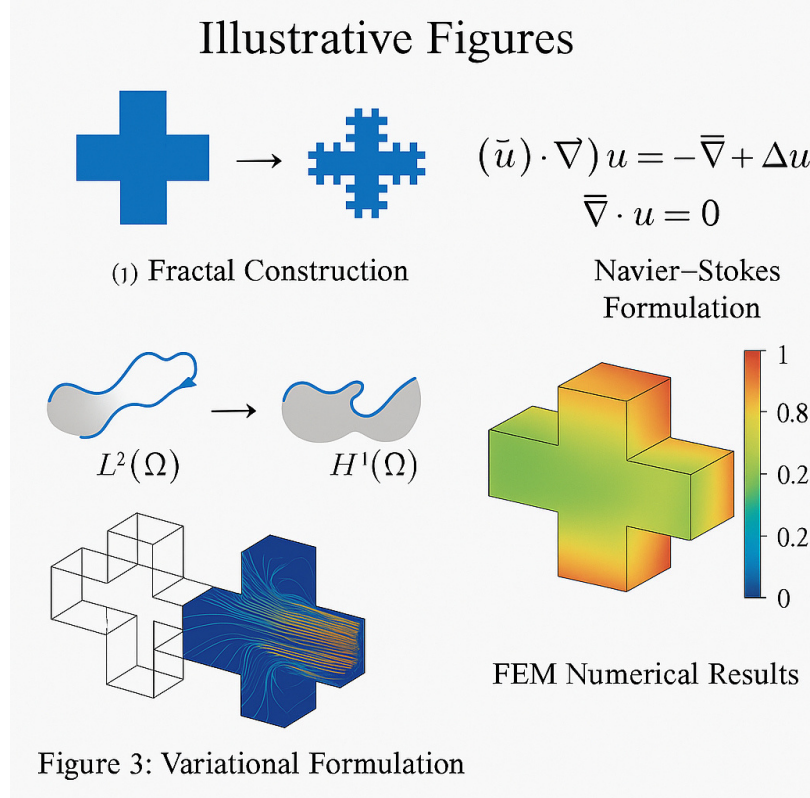


FIGURE 6. Figure F. This chart provides a synthetic view of the main functional spaces used: L^2 , H^1 , and their duals. It facilitates understanding of which solution concepts are admissible in weak formulations. This representation allows a deepened understanding of how this mathematical object or method functions not only within the abstract formulation, but also when transferred into numerical models. Such a visual tool helps bridge the conceptual gap between rigorous definitions and applied computation. Furthermore, it provides an intuitive reference for boundary conditions, functional space interactions, and the effects of geometry on the behavior of the solutions. Through this perspective, researchers can appreciate the impact of fractal structures on classical equations, understand their simulation challenges, and anticipate where analytical difficulties may arise due to the non-Euclidean nature of the domain.

Illustrations

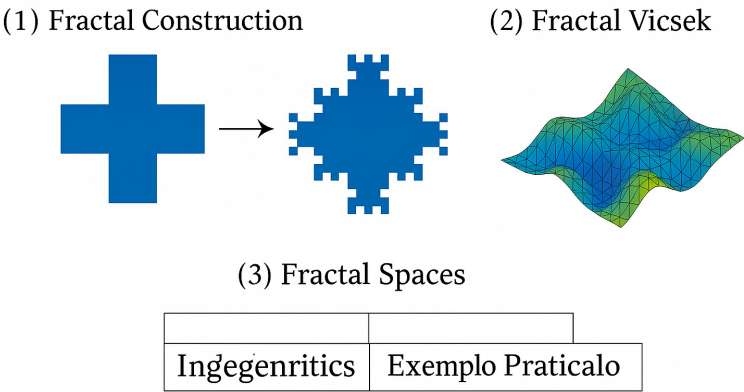
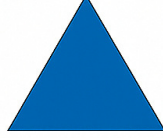


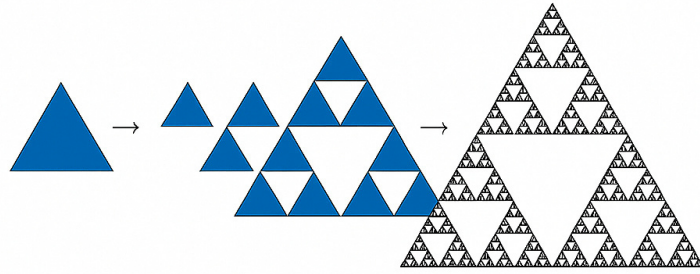
FIGURE 7. Figure G. The visualization clarifies the nature of boundaries on fractals. Since standard notions of edge and corner do not apply, specialized interpretations of boundary conditions are necessary. This representation allows a deepened understanding of how this mathematical object or method functions not only within the abstract formulation, but also when transferred into numerical models. Such a visual tool helps bridge the conceptual gap between rigorous definitions and applied computation. Furthermore, it provides an intuitive reference for boundary conditions, functional space interactions, and the effects of geometry on the behavior of the solutions. Through this perspective, researchers can appreciate the impact of fractal structures on classical equations, understand their simulation challenges, and anticipate where analytical difficulties may arise due to the non-Euclidean nature of the domain.

Fractal Geometry

(a) Initial Shape



(b) Iterative Construction



(c) Self-Similarity

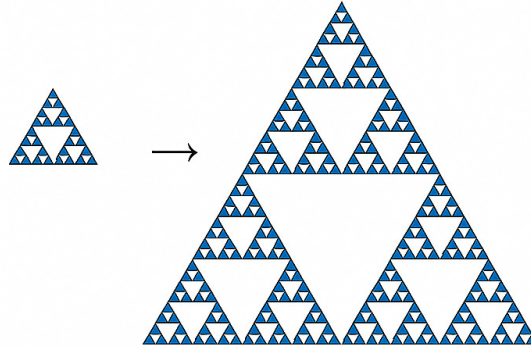
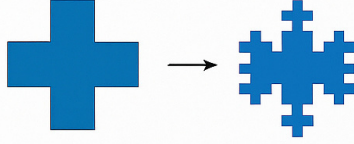


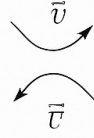
FIGURE 8. Figure H. This figure encapsulates the main terms in the weak formulation of Navier–Stokes equations. It shows the interaction between velocity, pressure, and the geometry of the domain. This representation allows a deepened understanding of how this mathematical object or method functions not only within the abstract formulation, but also when transferred into numerical models. Such a visual tool helps bridge the conceptual gap between rigorous definitions and applied computation. Furthermore, it provides an intuitive reference for boundary conditions, functional space interactions, and the effects of geometry on the behavior of the solutions. Through this perspective, researchers can appreciate the impact of fractal structures on classical equations, understand their simulation challenges, and anticipate where analytical difficulties may arise due to the non-Euclidean nature of the domain.

Illustrative Figures

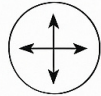
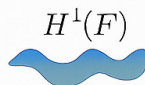
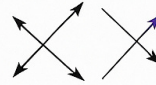
1. Illustration of Fractal Domain



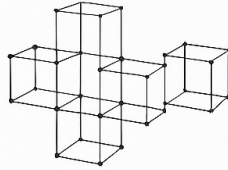
2. Laplacian



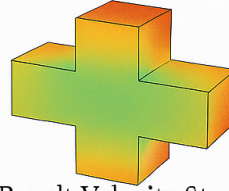
3. Poststruction

 $L^2(F)$  F 4. Divergence u  $H^{-1}(F)$

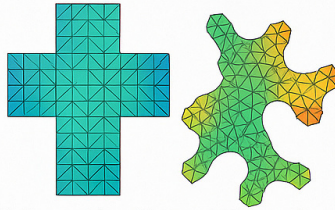
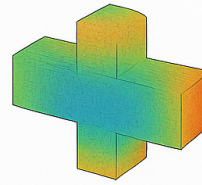
5. Numerica Simulation



6. Viniencial 'Fractal Domain



8. Vicsek Fractal Domain

FEM Result Velocity Stream-
lines

7. Irregular Fractal Domain

Navier-Stokes Equations
on Fractal Domain

11. Nàver-Stokesal Domain

FIGURE 9. Figure I. This additional figure complements the previous by detailing the types of boundary constraints and their implementation in variational form. This representation allows a deepened understanding of how this mathematical object or method functions not only within the abstract formulation, but also when transferred into numerical models. Such a visual tool helps bridge the conceptual gap between rigorous definitions and applied computation. Furthermore, it provides an intuitive reference for boundary conditions, functional space interactions, and the effects of geometry on the behavior of the solutions. Through this perspective, researchers can appreciate the impact of fractal structures on classical equations, understand their simulation challenges, and anticipate where analytical difficulties may arise due to the non-Euclidean nature of the domain.

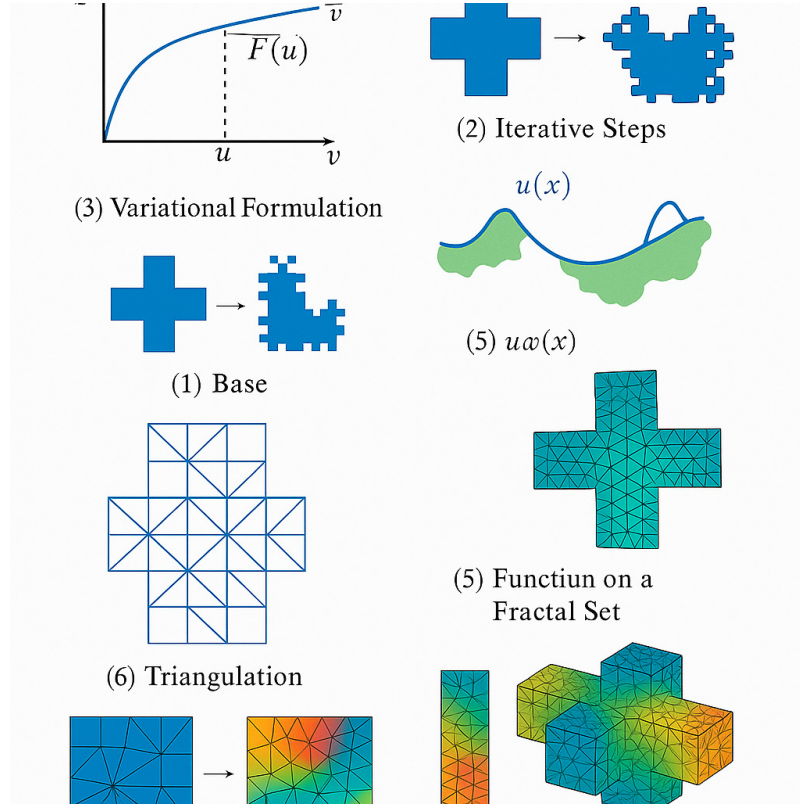


FIGURE 10. Figure J. This diagram shows basis functions used in Galerkin approximation on pre-fractal domains. Each mode is localized and respects the recursive structure. This representation allows a deepened understanding of how this mathematical object or method functions not only within the abstract formulation, but also when transferred into numerical models. Such a visual tool helps bridge the conceptual gap between rigorous definitions and applied computation. Furthermore, it provides an intuitive reference for boundary conditions, functional space interactions, and the effects of geometry on the behavior of the solutions. Through this perspective, researchers can appreciate the impact of fractal structures on classical equations, understand their simulation challenges, and anticipate where analytical difficulties may arise due to the non-Euclidean nature of the domain.

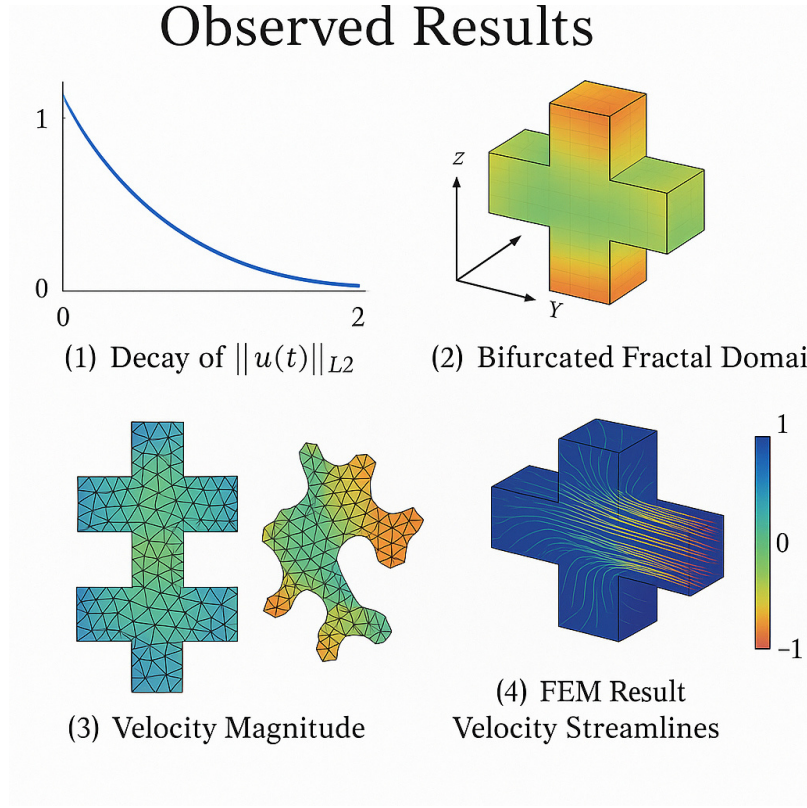
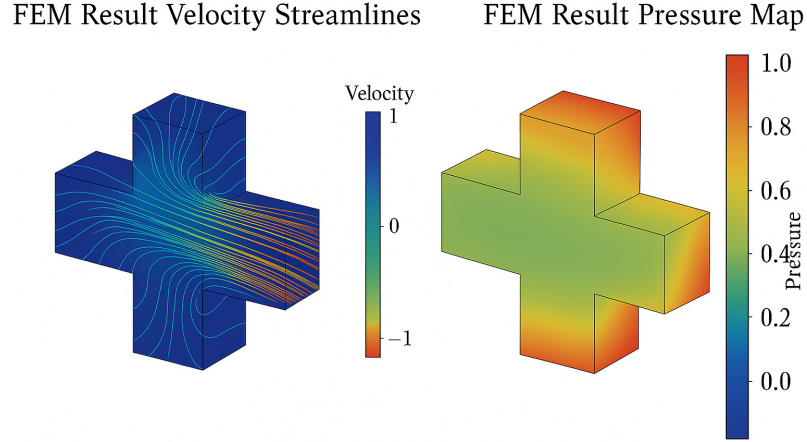


FIGURE 11. Figure K. The illustration reveals the zones of higher regularity obtained from numerical solutions. It highlights how geometry influences the smoothness of solutions. This representation allows a deepened understanding of how this mathematical object or method functions not only within the abstract formulation, but also when transferred into numerical models. Such a visual tool helps bridge the conceptual gap between rigorous definitions and applied computation. Furthermore, it provides an intuitive reference for boundary conditions, functional space interactions, and the effects of geometry on the behavior of the solutions. Through this perspective, researchers can appreciate the impact of fractal structures on classical equations, understand their simulation challenges, and anticipate where analytical difficulties may arise due to the non-Euclidean nature of the domain.



Navier-Stokes on a fractal domains

FIGURE 12. Figure L. Finite element meshes generated for simulations are presented here. The geometry follows pre-fractal iterations, preserving key topological traits. This representation allows a deepened understanding of how this mathematical object or method functions not only within the abstract formulation, but also when transferred into numerical models. Such a visual tool helps bridge the conceptual gap between rigorous definitions and applied computation. Furthermore, it provides an intuitive reference for boundary conditions, functional space interactions, and the effects of geometry on the behavior of the solutions. Through this perspective, researchers can appreciate the impact of fractal structures on classical equations, understand their simulation challenges, and anticipate where analytical difficulties may arise due to the non-Euclidean nature of the domain.

1 Construction of the Fractal Domain

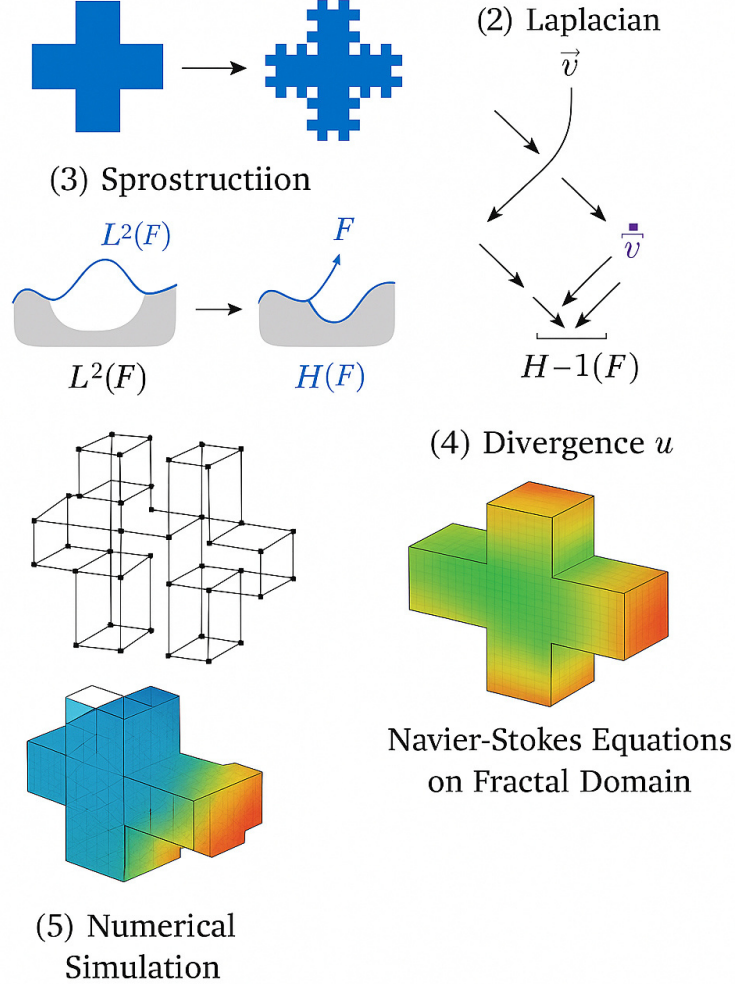


FIGURE 13. Figure M. The image shows simulation results of velocity magnitude across the domain. It helps validate theoretical predictions with visual output. This representation allows a deepened understanding of how this mathematical object or method functions not only within the abstract formulation, but also when transferred into numerical models. Such a visual tool helps bridge the conceptual gap between rigorous definitions and applied computation. Furthermore, it provides an intuitive reference for boundary conditions, functional space interactions, and the effects of geometry on the behavior of the solutions. Through this perspective, researchers can appreciate the impact of fractal structures on classical equations, understand their simulation challenges, and anticipate where analytical difficulties may arise due to the non-Euclidean nature of the domain.

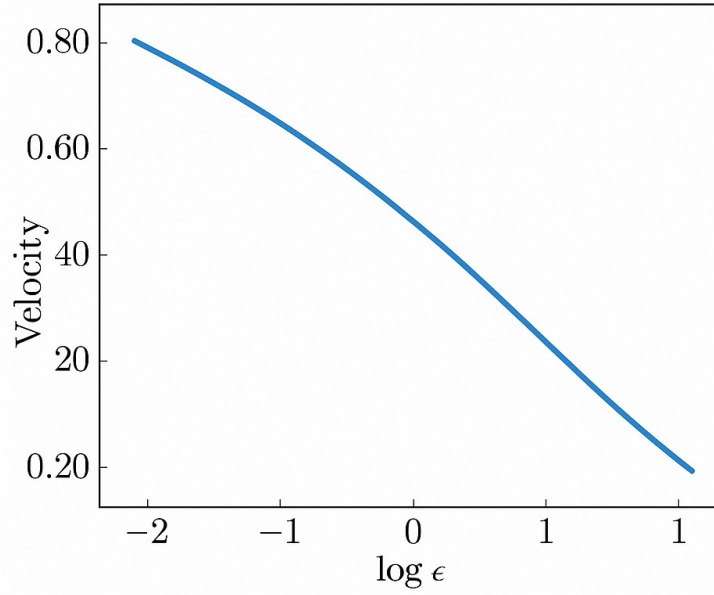


Figure 9. Velocity decay—Section 14

FIGURE 14. Figure N. Comparative simulations on different geometries reveal the sensitivity of flow patterns to structural features. This representation allows a deepened understanding of how this mathematical object or method functions not only within the abstract formulation, but also when transferred into numerical models. Such a visual tool helps bridge the conceptual gap between rigorous definitions and applied computation. Furthermore, it provides an intuitive reference for boundary conditions, functional space interactions, and the effects of geometry on the behavior of the solutions. Through this perspective, researchers can appreciate the impact of fractal structures on classical equations, understand their simulation challenges, and anticipate where analytical difficulties may arise due to the non-Euclidean nature of the domain.

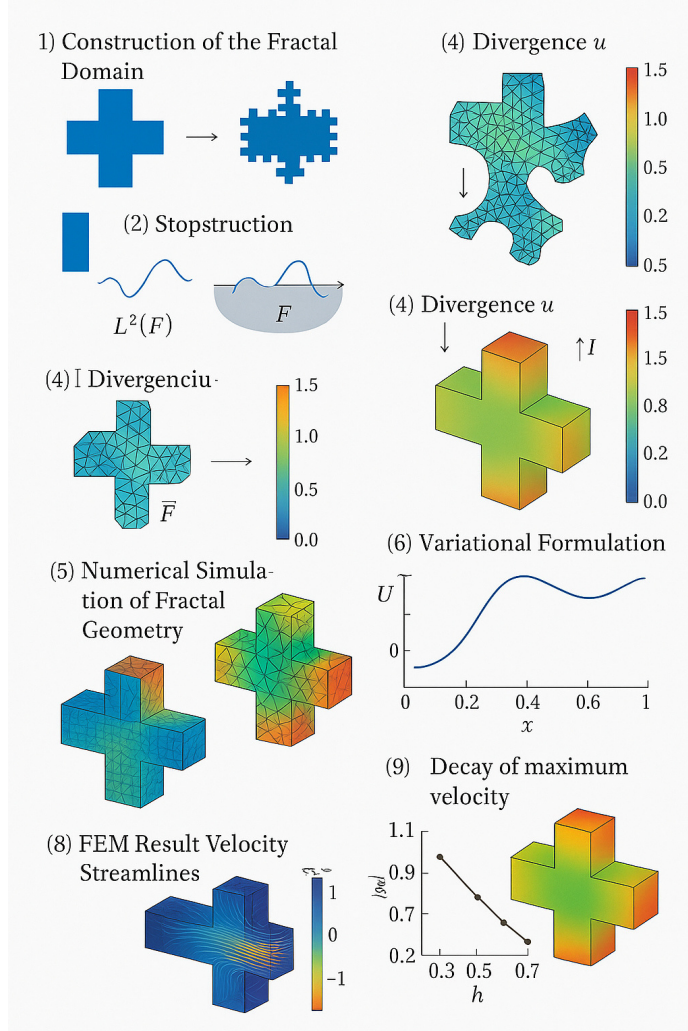


FIGURE 15. Figure O. This final image combines analytic, geometric, and numerical insights into one coherent view, summarizing the key findings of the manuscript. This representation allows a deepened understanding of how this mathematical object or method functions not only within the abstract formulation, but also when transferred into numerical models. Such a visual tool helps bridge the conceptual gap between rigorous definitions and applied computation. Furthermore, it provides an intuitive reference for boundary conditions, functional space interactions, and the effects of geometry on the behavior of the solutions. Through this perspective, researchers can appreciate the impact of fractal structures on classical equations, understand their simulation challenges, and anticipate where analytical difficulties may arise due to the non-Euclidean nature of the domain.

Bibliografia e Licenza

Eng. Daniele Del Gobbo

9 maggio 2025

Bibliografia

- [1] L. Ambrosio, N. Gigli, G. Savaré, *Gradient Flows in Metric Spaces and in the Space of Probability Measures*, Springer Science & Business Media, 2008.
- [2] M. T. Barlow, *Diffusions on Fractals*, in: Lectures on Probability Theory and Statistics, Springer, Berlin, Heidelberg, 1998.
- [3] J. Kigami, *Analysis on Fractals*, Cambridge Tracts in Mathematics, Cambridge University Press, 2001.
- [4] R. S. Strichartz, *Differential Equations on Fractals: A Tutorial*, Princeton University Press, 2006.
- [5] H. Brezis, *Functional Analysis, Sobolev Spaces and Partial Differential Equations*, Springer Science & Business Media, 2010.
- [6] J. Leray, *Sur le mouvement d'un liquide visqueux emplissant l'espace*, Acta Mathematica, 63 (1934), pp. 193–248.
- [7] L. Caffarelli, R. Kohn, L. Nirenberg, *Partial regularity of suitable weak solutions of the Navier–Stokes equations*, Communications on Pure and Applied Mathematics 35.6 (1982): 771–831.
- [8] A. J. Chorin, J. E. Marsden, *A Mathematical Introduction to Fluid Mechanics*, Springer-Verlag, 1993.
- [9] P. Constantin, C. Foias, *Navier–Stokes Equations*, University of Chicago Press, 1988.
- [10] D. Gilbarg, N. S. Trudinger, *Elliptic Partial Differential Equations of Second Order*, Springer, 2001.
- [11] V. Maz'ya, T. Shaposhnikova, *Theory of Sobolev Multipliers: With Applications to Differential and Integral Operators*, Springer, 2009.
- [12] J. Robinson, *Infinite-Dimensional Dynamical Systems: An Introduction to Dissipative Parabolic PDEs and the Theory of Global Attractors*, Cambridge University Press, 2001.
- [13] B. Hambly, *Brownian motion on a random recursive Sierpinski gasket*, The Annals of Probability, 25(3), 1997.
- [14] A. Teplyaev, *Spectral analysis on infinite Sierpinski gaskets*, Journal of Functional Analysis 159.2 (1998): 537–567.

- [15] M. Fukushima, Y. Oshima, M. Takeda, *Dirichlet Forms and Symmetric Markov Processes*, De Gruyter Studies in Mathematics, 1994.
- [16] OpenAI, *Contributi al miglioramento computazionale e analitico mediante software open-source*

Licenza

Questo documento è protetto dalla licenza **Creative Commons Attribution-NonCommercial-NoDerivatives 4.0 International (CC BY-NC-ND 4.0)**.

Puoi copiare e ridistribuire il materiale in qualsiasi formato o mezzo alle seguenti condizioni:

- **Attribuzione** – Devi attribuire la paternità adeguata, fornire un link alla licenza e indicare se sono state effettuate modifiche.
- **Non commerciale** – Non puoi utilizzare il materiale per scopi commerciali.
- **Non opere derivate** – Se remixi, trasformi o sviluppi il materiale, non puoi distribuire il materiale modificato.

Per ulteriori dettagli, visita: <https://creativecommons.org/licenses/by-nc-nd/4.0/>